Harmonic and Two-Tone Intermodulation Distortion Analyses of the Inverted InGaAs/InAlAs/InP HBT

Bin Li and Sheila Prasad

***Abstract*—Harmonic and two-tone intermodulation distortion analyses of the InGaAs/InAlAs/InP collector-up heterojunction bipolar transistor (HBT) are performed by a simple Ebers–Moll model. The parasitic elements of the equivalent circuit are extracted at zero bias by numerical optimization. A semianalytical approach is used to extract the intrinsic parameters of the small-signal equivalent circuit at nonzero bias points. Appropriate equations given by device physics are fitted to the bias variation of intrinsic parameters so that the Ebers–Moll model parameters can be extracted. Agreement between simulation and measurement of harmonic and intermodulation distortion is achieved.**

***Index Terms*—Distortion, heterojunction bipolar transistor (HBT), intermodulation.**

I. Introduction

Heterojunction bipolar transistors (HBT's) are presently used in many analog and digital applications. Although small-signal models for the HBT's have been developed extensively, the same is not true for large-signal HBT models. Several models, including the numerical model, the conventional Gummel–Poon model, and the modified Ebers–Moll model have been presented in [1]. Large-signal HBT modeling is an ongoing effort, since this model is essential for most practical applications [2]–[4].

This paper presents a simple Ebers–Moll model based on the quasi-static technique which makes use of multibias scattering parameters and dc measurements to extract a bias-dependent nonlinear equivalent circuit model. The Ebers–Moll model is more accurate than the Gummel–Poon model since it includes the transit time effects [1]. Section II gives the small-signal equivalent circuit of the collector-up HBT and the method of extracting the small-signal parameters. The bias-dependent intrinsic elements are also identified. The equations governing the nonlinearity of the intrinsic elements and the method of extracting the parameters of the Ebers–Moll model are given in Section III. The comparison of simulation and measurement of harmonic distortion, as well as the two-tone third-order intermodulation distortion, is given in Section IV.

II. Small-Signal Model of Collector-Up HBT

The device under investigation is a 5×10 μm^2 InGaAs/InAlAs/InP-inverted HBT with $f_T = 23$ GHz and $f_{\max} = 20$ GHz. The small-signal equivalent circuit of the device [5], [6] is shown in Fig. 1. There is no base collector feedback capacitor in the inverted HBT. L_b, L_c, L_e, $C_{\rm pbe}$, $C_{\rm pbc}$, and C_{pce} are parasitic inductances and capacitances, respectively, R_b, R_c, and R_e are extrinsic resistances. The active portion of the HBT is modeled by intrinsic elements C_e, r_e, C_{jc}, α, and R_{jc}, where $\alpha = \frac{\alpha_F}{1+jf/f\alpha} e^{-j\omega\tau}$. α_F is the dc value of the transport factor, τ is the transit time of collector current, and f_α is an α 3-dB frequency. RF measurements indicate that the HBT under zero bias ($I_b = 0\,A, V_{CE} = 0$ V) can be represented by a passive network. Therefore, in this case, the transport factor α is negligible. Moreover, the dynamic resistance of the base–collector $p-n$ junction and the base–emitter $p-n$ junction is assumed to be very large. The uncertainty of numerical optimization in zero bias can be reduced. The initial values that are assumed in optimization are calculated from the physical and geometrical parameters. The parasitic elements, $C_{\rm pbe}$, $C_{\rm pbc}$, C_{pce}, L_b, L_e, and L_c, are obtained from zero-bias numerical optimization and assumed to be invariant with bias [6]. Their values are listed in Table I.

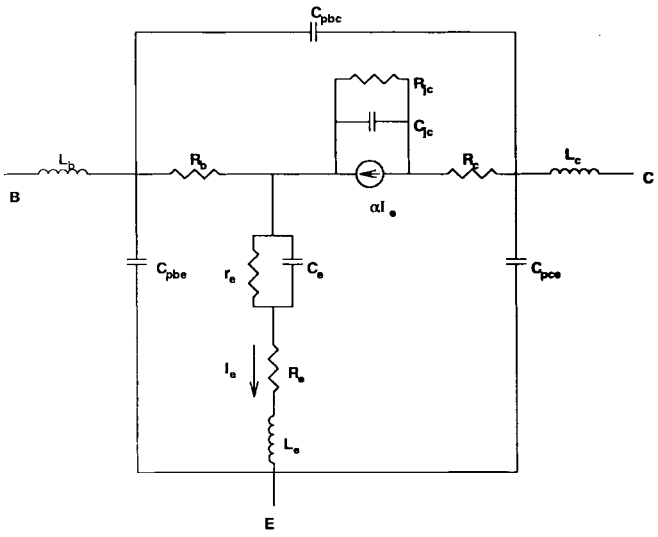

Fig. 1. Small-signal equivalent circuit of the inverted HBT.

The other elements under nonzero bias are extracted by the following analytical approach:

- convert the s-parameters to z-parameters and remove the parasitic series elements L_b and L_c;
- convert the z-parameters to y-parameters and remove the parasitic shunt elements C_{pbe}, C_{pce}, C_{pbc};
- convert the y-parameters to h-parameters.

The elements of the equivalent circuit, excluding the parasitic effects, are easily extracted using the procedure described in [7].

The elements R_b, L_e, R_e, and R_c are basically constant over the entire frequency range of interest and do not show significant variation with bias. Therefore, these elements can be considered to be fixed. The bias-dependent elements are C_e, C_{jc}, R_{jc}, α_F, τ, $f\alpha$, and r_e. It has been shown that the consideration of the bias variation of these elements is sufficient for accurate small-signal modeling [5], [6].

III. Large-Signal Model

The large-signal equivalent circuit is shown in Fig. 2. For the large-signal model, the following equations are used to characterize the intrinsic elements

$$r_e = \frac{n_{be} k R}{qIe} \tag{1}$$

$$C_e = C_{je} + \tau_F / r_e \tag{2}$$

$$C_{jc} = C_{jc0}(1 - V'_{bc}/V_{jc0})^{-M_{jc}} \tag{3}$$

$$C_{je} = C_{je0}(1 - V'_{be}/V_{je0})^{-M_{je}} \tag{4}$$

Manuscript received July 23, 1996; revised March 24, 1997. The work of S. Prasad was supported in part by Advanced Research Projects Agency under Grant ONR/N00014-94-1-0687.

The authors are with the Department of Electrical and Computer Engineering, Northeastern University, Boston, MA 02115 USA.

Publisher Item Identifier S 0018-9480(97)04467-0.

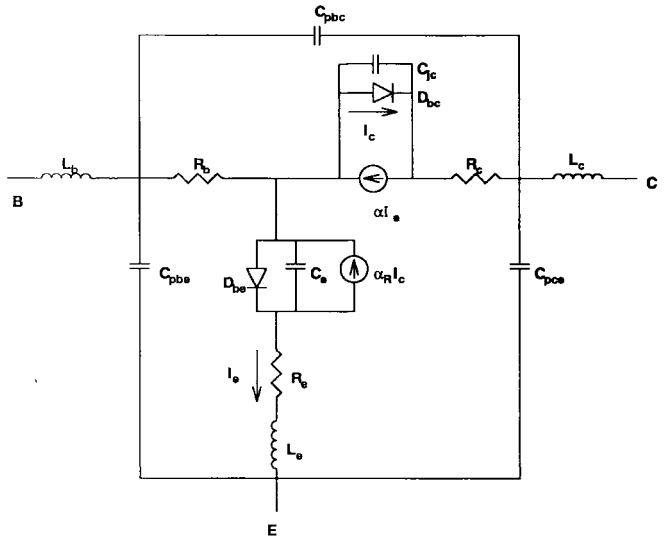

Fig. 2. Large-signal equivalent circuit of the inverted HBT.

$$I_e = I_{sR}(e^{qV'_{bc}/n_{bc}kT} - 1) \text{ at } V_{be} = 0 \quad (5)$$

$$I_c = I_{sF}(e^{qV'_{be}/n_{be}kT} - 1) \text{ at } V_{bc} = 0 \quad (6)$$

$$\alpha_F I_{SF} = \alpha_R I_{sR}. \quad (7)$$

The description of the symbols is given in Table I. Equations (1)–(7) are given by device physics [8] and the corresponding currents and voltages are those of the intrinsic device. In the small-signal device model, the plot of $(R_e + r_e)$ versus $1/I_e$ is used to extract n_{be} [1] (shown in Fig. 3). τ_F is extracted from (2). C_{jeo}, C_{jc0}, V_{je0}, V_{jc0} are extracted from (3)–(4) by fitting them to bias-dependent intrinsic capacitance elements. M_{je} is assumed to be 0.5 for the abrupt emitter–base junction. M_{jc} is assumed to be 0.33 for the graded base–collector junction. I_{sR} and n_{bc} are extracted from the inverse Gummel–Poon curve. I_{sF} is extracted from forward Gummel–Poon curve. The transit time of collector current τ is incorporated in the frequency dependence of α. α_R is obtained from (7). The variation of α (α_0, f_α, τ) with bias is not included in the present model. α_0, f_α, and τ at the applied bias are used for simulation in the overall power excitation range.

During dc measurements, the base current I_b and collector-emitter voltage V_{ce} are applied, the base–emitter voltage V_{be} and collector current I_c are measured. Given the extrinsic values of voltage and current, the intrinsic base–collector voltage, base–emitter voltage, and emitter current are defined by the following equations:

$$I_e = I_c + I_b \quad (8)$$

$$V'_{be} = V_{be} - I_e R_e - I_b R_b \quad (9)$$

$$V'_{bc} = V_{bc} - I_b R_b + I_c R_c. \quad (10)$$

Equations (8)–(10) are used to fit the bias variations of the intrinsic element values and the corresponding parameters of the model are determined. The model parameters are listed in Table I.

IV. Simulation of Harmonic Distortion

A large-signal equivalent-circuit model has been developed using LIBRA [9]. The harmonic distortion analysis has also been performed. The simulation was performed at 6 GHz with $V_{ce} = 1.2$ V and $I_b = 150$ μA corresponding to an $I_c = 4.5$ mA. Fig. 4 shows the measured and simulated fundamental and second harmonics. The maximum deviations between measurement and simulation are as follows: 0.4 dB for the fundamental and 3 dB for the second harmonic.

TABLE 1
Ebers–Moll Model Parameters for the Inverted HBT

Component	Value	Description
L_b	30 pF	parasitic base inductance
L_c	49 pF	parasitic collector inductance
L_e	10 pF	parasitic emitter inductance
C_{pbc}	40 fF	parasitic base-emitter capacitance
C_{pce}	31 fF	parasitic collector-emitter capacitance
C_{pbc}	6.3 fF	parasitic base-collector capacitance
R_b	170 Ω	extrinsic base resistance
R_c	17 Ω	extrinsic collector resistance
R_e	50 Ω	extrinsic emitter resistance
I_{sF}	1e-16 A	BE junction saturation current
n_{bc}	1.04	BE junction ideality coefficient
M_{jc}	0.5	BE junction grading coefficient
V_{je0}	1.8 V	BE junction potential
C_{je0}	1.3e-13 F	BE zero-bias junction capacitance
τ_F	3 ps	BE junction diffusion time
I_{sR}	4.5e-6 A	BC junction saturation current
n_{bc}	2.84	BC junction ideality coefficient
M_{jc}	0.33	BC junction grading coefficient
V_{jc0}	1.95 V	BC junction potential
C_{jc0}	3.3e-14 F	BC junction zero-bias capacitance
α_F	0.92	dc value of transport factor
f_α	24 GHz	α_F 3 dB frequency
τ	5 ps	forward transit time delay
α_R	2.25e-11	inverse transport factor

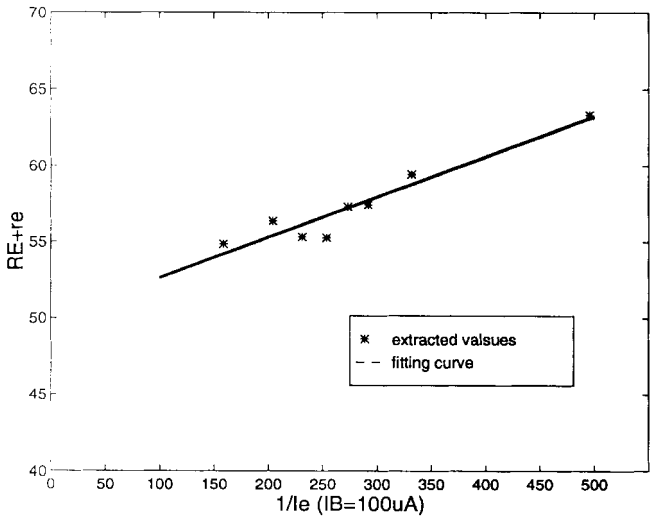

Fig. 3. $R_e + r_e$ versus $1/I_e$.

This investigation also indicates that the transit time delay τ and base–emitter junction-ideality coefficient have a significant effect on the simulated results. In the simulation, the source impedance and load impedance are assumed to be 50 Ω. The source and load

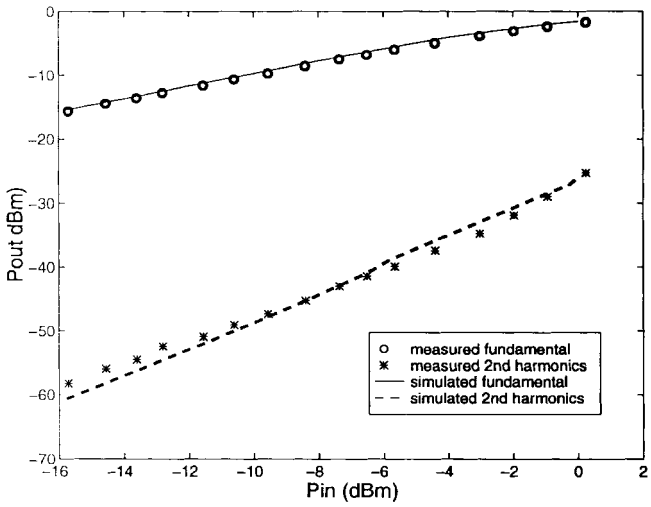

Fig. 4. The measured and simulated harmonic-distortion result of the inverted HBT at $V_{ce} = 1.2$ V, $I_b = 150$ μA.

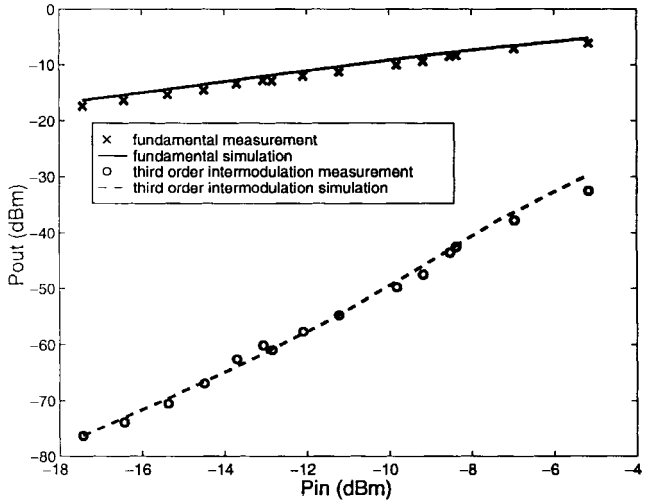

Fig. 5. Two-tone third-order intermodulation distortion of the inverted HBT at $V_{ce} = 1.5$ V, $I_b = 170$ μA.

impedances at fundamental and second harmonic frequencies are also measured. Simulation results with the measured impedances do not show significant differences.

The two-tone third-order distortion simulation is performed to verify the resulting HBT model. The harmonic-balance simulator in LIBRA[1] was used in this simulation. Fig. 5 shows the measured and simulated distortion at the bias of $V_{\rm ce} = 1.5$ V, $I_b = 170$ μA. A bias point different from that used in harmonic-distortion analysis is chosen to verify the validity of the proposed model. Both bias points are for class AB power application. The two fundamental signal frequencies are 6.02 and 6.08 GHz, respectively. The third-order intermodulation distortions are average at 5.96 and 6.14 GHz. The source and load impedances are again assumed to be 50 Ω. The difference between simulation and measurement is well within 1.5 dBm.

[1] HPEEsof, Westlake Village, CA, *Libra, series 4.0*, 4.0 ed.

V. Conclusion

A simple Ebers–Moll model for predicting the nonlinear performance of the inverted HBT has been presented. It is based on the experimental characterization of the frequency and bias-dependent behavior of the device small-signal s-parameters. The model parameters are deduced by fitting the bias-dependent intrinsic elements to the underlying equations from physics. The good agreement between measurement and simulation of harmonic and two-tone intermodulation distortions shows that this simple Ebers–Moll model is valid and useful in applications where nonlinearity is important. It avoids the complexity of the Gummel–Poon model, while the requirement of good agreement between measurement and simulation can be satisfied.

Acknowledgment

The authors wish to thank Dr. B. Meskoob for providing his measurement data. They also wish to thank Prof. C. G. Fonstad of the Massachusetts Institute of Technology for providing the devices and the use of laboratory facilities for this research.

References

[1] D. A. Teeter, J. R. East, R. K. Mains, and G. I. Haddad, "Large-signal numerical and analytical HBT models," *IEEE Trans. Electron Devices*, vol. 40, pp. 837–845, May 1993.

[2] P. C. Grossman and J. Choma, "Large-signal modeling of HBT's including self-heating and transit time effects," *IEEE Trans. Microwave Theory Tech.*, vol. 40, pp. 449–464, Mar. 1992.

[3] M. Y. Frankel and D. Pavlidis, "An analysis of the large-signal characteristic of AlGaAs/GaAs heterojunction bipolar transistors," *IEEE Trans. Microwave Theory Tech.*, vol. 40, pp. 465–474, Mar. 1992.

[4] K. Wu and P. A. Perry, "A new large-signal AlGaAs/GaAs HBT model including self-heating effects, with corresponding parameter-extraction procedure," *IEEE Trans. Microwave Theory Tech.*, vol. 43, pp. 1433–1445, July 1995.

[5] B. Meskoob, S. Prasad, M. Vai, J. Vlcek, H. Sato, C. G. Fonstad, and C. Bulutay, "A small-signal equivalent circuit for the collector-up InGaAs/InAlAs/InP heterojunction bipolar transistor," *IEEE Trans. Electron Devices*, vol. 39, pp. 2629–2632, Nov. 1992.

[6] B. Meskoob, S. Prasad, M. Vai, J. C. Vlcek, H. Sato, and C. G. Fonstad, "Bias-dependence of the intrinsic element values of InGaAs/InAlAs/InP inverted heterojunction bipolar transistor," *IEEE Trans. Microwave Theory Tech.*, vol. 40, pp. 1012–1014, May 1992.

[7] D. R. Pehlke and D. Pavlidis, "Evaluation of the factors determining HBT high-frequency performance by direct analysis of s-parameter data," *IEEE Trans. Microwave Theory Tech.*, vol. 40, pp. 2367–2373, Dec. 1992.

[8] S. M. Sze, *Physics of Semiconductor Devices.* New York: Wiley, 1981.